



Article

Novel Approach to Respiratory Rate Measurement Using Resonance Tube with Contradictory Thresholding Technique

Trizit Benjaboonyazit^{1,a}, Mana Sriyudthsak^{2,b,*}, Tayard Desudchit^{3,c},
and Kwanrat Suanpong^{4,d}

¹ Technopreneurship and Innovation Management Program, Graduate School, Chulalongkorn University, Bangkok 10330, Thailand

² Department of Electrical Engineering, Faculty of Engineering, Chulalongkorn University, Bangkok 10330, Thailand

³ Division of Pediatric Neurology, Department of Pediatrics, Faculty of Medicine, Chulalongkorn University, Bangkok 10330, Thailand

⁴ Chulalongkorn Business School, Chulalongkorn University, Bangkok 10330, Thailand

E-mail: ^aTriZit@gmail.com, ^bMana.S@chula.ac.th (Corresponding author), ^cTayard.D@chula.ac.th,

^dKwanrat@cbs.chula.ac.th

Abstract. In this paper, we propose a novel approach to respiratory rate measurement using resonance tube to enhance the performance of microphone inserted and fixed at the end of the tube to catch breath sound signal from the mouth and/or nose. The signal is amplified and passed into envelope detector circuit after which it is compared with a suitable reference voltage in comparator circuit to generate a pulse train of square wave synchronized with the respiratory cycle. A simple algorithm is developed in a small microcontroller to detect rising edges of each consecutive square wave to calculate respiratory rate together with analysis of breathing status. In order to evade noises which will cause errors and artifacts in the measuring system, the reference voltage is creatively designed to intelligently adapt itself to be low during expiration period and high during inspiration and pause period using the concept of resolving contradiction in the theory of inventive problem solving (TRIZ). This makes the developed device simple and low-cost with no need for complicated filtering system. It can detect breath sound as far as 250 cm from the nose and can perform accurately as tested against End Tidal CO₂ Capnography device. The result shows that the developed device can estimate precisely from as low as 0 BrPM to as high as 98 BrPM and it can detect shallow breathing as low as 10 mV of breath sound.

Keywords: Respiratory rate, medical device, resonance tube, microphone, TRIZ.

ENGINEERING JOURNAL Volume 23 Issue 6

Received 7 February 2019

Accepted 25 October 2019

Published 30 November 2019

Online at <http://www.engj.org/>

DOI:10.4186/ei.2019.23.6.361

1. Introduction

Respiratory rate is one of the important vital signs besides pulse rate, blood pressure and body temperature [1]. An abnormal respiratory rate can be a significant indicator of serious illness such as cardiac arrest [2]. Respiratory rate monitoring plays an important role in intensive care unit (ICU) [3] and is one of the fundamental indicators in sleep study (polysomnography) [4]. Furthermore, as people become more health conscious nowadays, practices of mindfulness using breathing become more widespread as it is believed to be the best tool for maintaining good health both physically and mentally [5]. There have been several researches on various kinds of methods and technologies developed to measure respiratory rate using parameters changes in the physical, chemical or biological elements inside and outside the body of human that are caused by respiration activities [6]. For example, changes in the impedance of the chest or abdomen, changes in the temperature, pressure or humidity of the inhaled and exhaled air, or changes in the CO₂ level in the end tidal airflow. Many sophisticated technologies have been developed to measure respiratory rate in accordance with each method, such as impedance pneumography [7], respiratory inductance plethysmography or RIP [8] and capnography using non-dispersive infrared end tidal CO₂ sensor, etc [9].

Another common method of measuring respiratory rate is to catch respiratory sound using microphone. This method is mostly used in the analysis of pulmonary disease based on lung sounds acquired by attaching microphone sensor to the skin on the chest or trachea on the neck. Normal frequency of pulmonary or lung sounds usually varies from 100 to 1000 Hz [10]. These lung sounds are prone to noises from heart sound and artefact from body movements where complicated noise filtering system is required [11]. In contrast to lung sounds, respiratory sound directly measured at the mouth is referred as breath sound by Forgacs who found that breath sounds recorded through a microphone close to the mouth contain sound waves of random amplitude with frequency distribution between about 200 and 2,000 Hz and breath sound of a healthy person at rest is barely audible at the mouth, while in chronic bronchitis or asthma, it is very noisy [12]. However, breath sounds at the mouth have attracted virtually no further investigational attention since the early 1970s [13] due to its nature of being weak signal and being susceptible to noise.

This paper aims to investigate the possibility of using breath sound for measuring respiratory rate and propose a new approach for measuring respiratory rate by deploying resonance tube to enhance the performance of the microphone system to catch breath sound at the mouth and/or nostril. Simple signal pre-processing procedure and data analysis algorithm with no complicated noise filtering system is developed. The prototype of the new system is designed, fabricated and tested with satisfactory result as detailed in the following sections.

2. Methodology

The respiratory rate monitoring device developed in this paper uses resonance tube to enhance the performance of the microphone system in catching breath sound and also uses TRIZ concept of Physical Contradiction and The Principle of Separation to solve the problem of the contradictory requirement of reference voltage in the comparator circuit to evade noises and thus improve the accuracy of measurement. Therefore, this section will give a basic knowledge of the phenomenon of stationary wave in resonance tube and TRIZ concept of Physical Contradiction, and explain how the respiratory rate monitoring device works.

2.1. Phenomenon of Stationary Wave in Resonance Tube

Sound propagates as a longitudinal wave with the normal velocity at 343 m/s. When travelling through a closed end tube, the sound wave will reflect at the closed end, causing it to resonate at a resonance frequency which depends on the length of the tube. Sound travels as a compression wave, causing air molecules to move back and forth along the direction of propagation. Within a tube, a stationary wave is formed. At the closed end of the tube, air molecules cannot move freely, making it a displacement node in the standing wave. And at the open end of the tube, air molecules can move with no restriction, making it a displacement antinode. When blowing sound into the tube, a frequency that matches one of the harmonic standing waves of the tube will

resonate, giving a maximum sound pressure at the resonance frequency. The reinforcement of power is due to synchronized reflection of the wave as shown in Fig. 1.

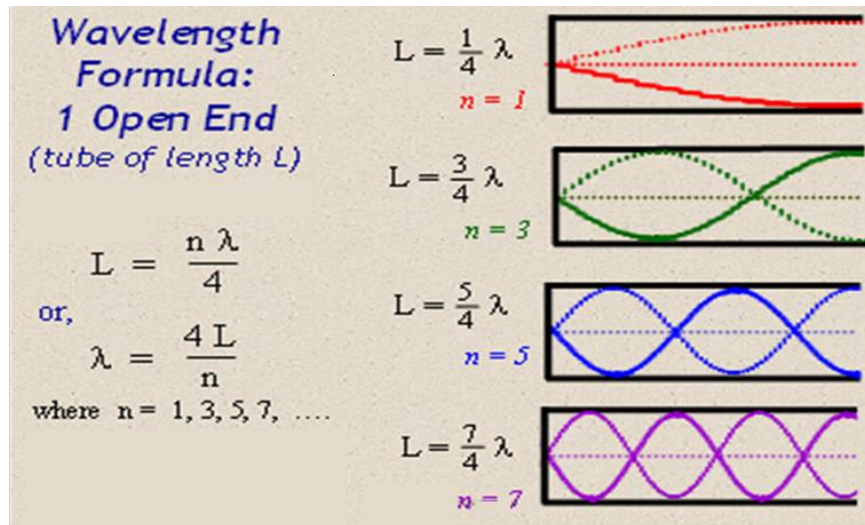


Fig. 1. Phenomenon of stationary wave in resonance tube with one open end.

(Source: <http://www.sliderbase.com/spitem-1610-9.html>)

Figure 1 shows that the standing wave in the resonance tube with one open end will occur only at the odd harmonic frequency. The fundamental frequency as the function of the length of the tube can be calculated as $f_1 = 1/(4L)$ Hz or wave length $\lambda = 4L$ where L is the length of the tube. And there occurs also the resonance of the odd harmonic frequency which is the odd number time of fundamental frequency as $f_3 = 3/(4L)$, $f_5 = 5/(4L)$, $f_7 = 7/(4L)$... and the wavelength of the harmonic frequency can be calculated as $\lambda = 4L/n$, where $n = 1, 3, 5, 7, \dots$. The frequency will be equal to velocity of sound divided by wave length or $f = v/\lambda$ Hz.

2.2. TRIZ concept of Physical Contradiction and the Principle of Separation

TRIZ is the Russian acronym for the Theory of Inventive Problem Solving developed by Genrikh Altshuller in 1946 who studied thousands of patents to discover how inventors innovated. In TRIZ, there are two main types of inventive problems. One is technical contradictions which occurs when two different parameters in a system conflict with each other. For example, a system could be stronger but at the cost of weight of the system. The second main type of inventive problems is physical contradictions where a system has contradictory requirements so that one parameter within the system conflicts with itself. For example, a pen tip needs to be sharp to write fine lines, but blunt in order to avoid damaging the paper it is writing on.

Physical contradiction underlies the root cause of problems and can be resolved through the use of the Principle of Separation by considering each of the 4 directions as follows:

- 1) Separation in time: Changing a property, response, behaviour against time
- 2) Separation in space: Changing the property, response, or behaviour based on special location
- 3) Separation between parts and the whole: Changing the property so as to make it different in the sub-system, system and/or super-system.
- 4) Separation upon condition: Changing the property of the contradictory element so as to make it different under different condition.

This paper deploys TRIZ concept of Physical Contradiction and the Principle of Separation as will be demonstrated in the following section.

2.3. Respiratory Rate Monitoring Device Using Resonance Tube

The respiratory rate monitoring device developed in this paper consists of 3 parts, breath sound signal acquisition unit, signal pre-processing unit, and data analysis and display unit as shown in Fig. 2.

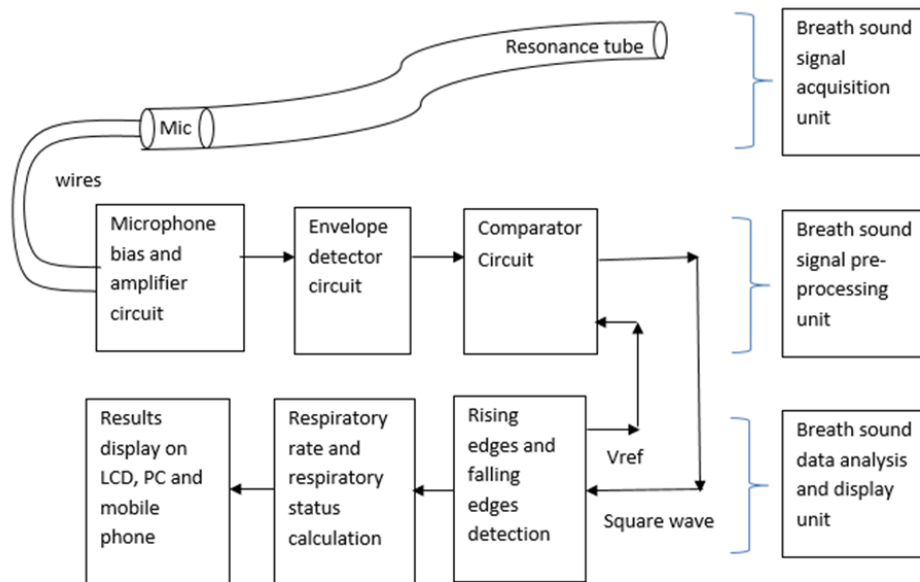


Fig. 2. Respiratory rate monitoring device using resonance tube.

Breath sound signal acquisition unit is made of a flexible tube, called here as resonance tube as of its function. A small electret condenser microphone is inserted and fixed at one end of the tube while the other end is placed near the mouth and/or nostril. Breath sound will travel inside the tube as longitudinal wave and will cause resonance inside the tube with resonance frequency that changes with the length of the tube. The breath sound in the resonance tube will transform into electrical signal through the microphone and will pass into the signal pre-processing unit which will amplify and detect the envelope of the signal. The envelope of the signal will then pass into the comparator circuit which will compare the envelope of the signal with suitable reference signal to generate a pulse train of square wave which is synchronized with the respiratory cycle. The data analysis and display unit is made of a microcontroller which is programmed to detect the rising edges of two consecutive square wave pulse after which respiratory rate will be calculated and displayed continuously on LCD and/or smart phone wirelessly. Furthermore, the data analysis and display unit will analyze respiratory rate at each respiratory cycle and show the respiratory status related to that respiratory rate as in Table 1.

Table 1. Respiratory status related to respiratory rate.

respiratory rate (BrPM)	respiratory status	Note
BrPM > 20	Tachypnea	Fast breathing
12 ≤ BrPM ≤ 20	Eupnea	Normal Breathing
6 ≤ BrPM < 12	Bradypnea	Slow Breathing
0 < BrPM < 6	Apnea	No breathing longer than 10 seconds
BrPM = 0	No breathing	No breathing longer than 60 seconds

3. Experiments and Results

Experiments are carried out to test each unit and the entire system, and the results are shown as follows:

3.1. Breath Sound Signal Acquisition Unit

Breath sound is acquired through the resonance tube with microphone inserted and fixed at one end. The experiment will compare the performance of microphone with and without resonance tube.

3.1.1. Experimental setup

A small electret condenser microphone (obopro2, diameter 6.0 mm) is used as a sensor fixed inside one end of a flexible tube with the same diameter and the tube length is divided between about 3 to 160 cm. The frequency response is between 20-16,000 Hz and the operating voltage of the microphone is between 1.1 - 10 V (Model no. OBO-62SN-0B-012, Source: <http://pro2inc.com>). The microphone is connected to the microphone socket of a notebook with audio software (Audacity 2.2.2) installed in it for displaying amplitude of breath sound signal in time domain, spectrum plot and time-frequency spectrogram. The sound signal in time domain represents the sound pressure level of breath sound which is then converted to a voltage level through the microphone bias circuit. This voltage is amplified and later digitized by the ADC within the computer audio interface circuit. This digital signal is then read and displayed as the sound waveform in the Audacity output display screen and normalized to within the limit of ± 1 level. The gain can be adjusted by the recording volume so that the signal (input to the ADC) will stay within these limits and therefore will not be further distorted. For frequency analysis, the Audacity software utility has the option to convert the sound signal in time domain to frequency domain and display it in the form of power spectrum with the horizontal scale in Hz and the vertical scale in dB. The dB shown in spectrum plot is of zero or negative values as the sound pressure values in time domain lie between +1 and -1. Another display option is the time-frequency spectrogram which will display the variation of frequency and power spectrum in vertical axis along with time in horizontal axis. The spectrum of power variation is displayed with range of colors starting from yellow, red, blue, and white showing from high to low power intensity. The microphone level is set to 100 % and 0 dB boost; the sampling rate is 44100 Hz, and the window function is Hanning window with the size of 1024 as shown in Fig. 3.

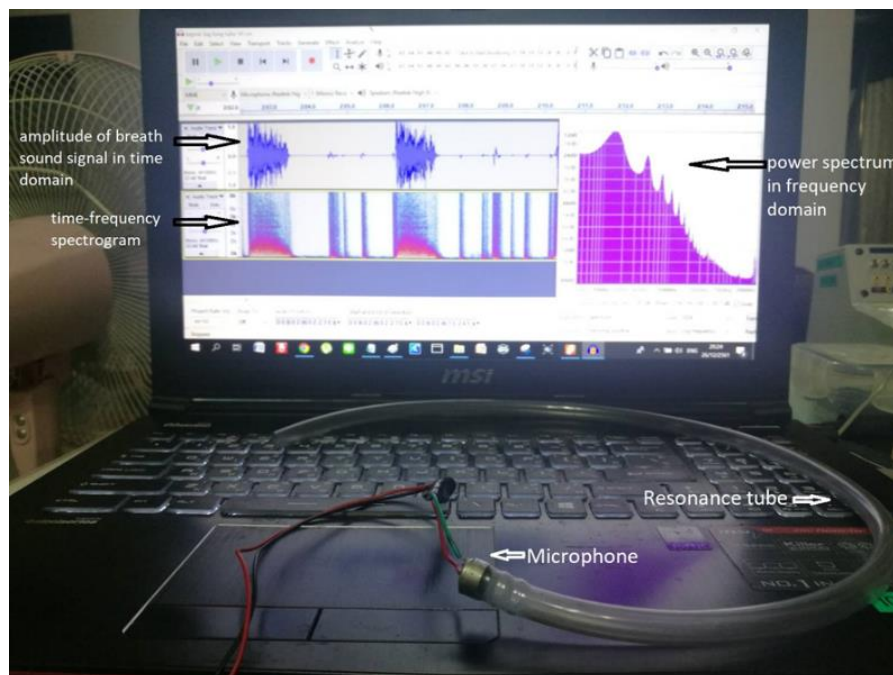


Fig. 3. Experimental setup for breath sound signal acquisition unit.

In another separate experiment, a microphone with no attached resonance tube is also placed in front of the nostril with distance from 1 to 15 cm to evaluate the dB at 100 Hz in order to compare with the performance of the microphone with resonance tube.

For both experiments, normal breathing air is blown from the nostril of a volunteer into the microphone directly and into the open end of the resonance tube separately, keeping the sound pressure level as constant as possible.

3.1.2. Experimental result

For microphone performance testing without resonance tube, no resonance is detected in spectrum plot and time-frequency spectrogram as the example shown in Fig. 4.

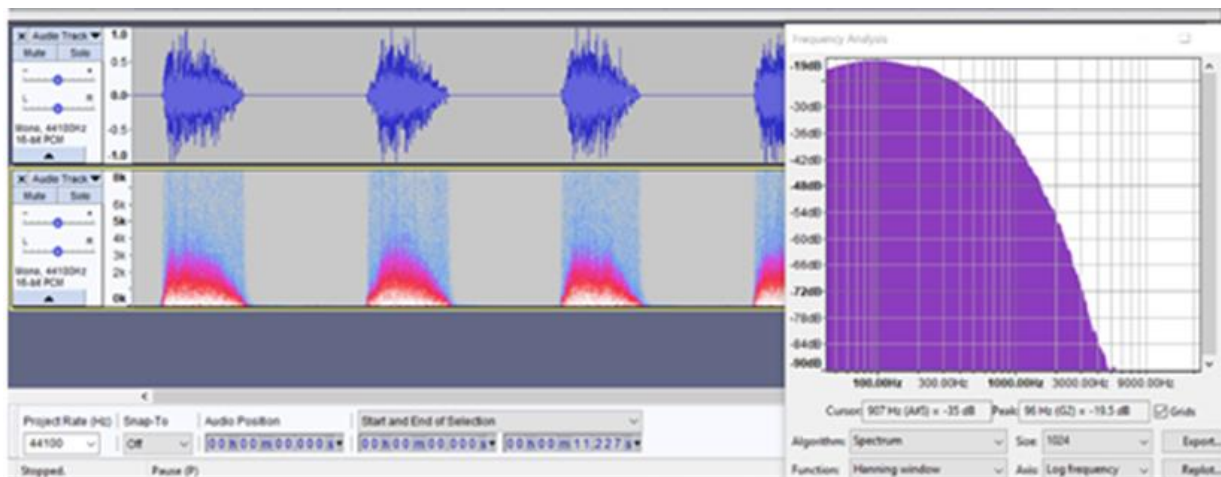


Fig. 4. Typical example of spectrum plot of microphone with no resonance tube (distance 3 cm from the nostril).

Figure 4 shows that without resonance tube, the frequency range of the spectrum plot of breath sound is between 40- 5,000 Hz. The maximum dB is around 100 Hz and it will drop significantly after 2,000 Hz. For the purpose of comparison, the dB at 100 Hz is selected from spectrum plot for different distance of the microphone from the nostril and the result is shown in Fig. 5.

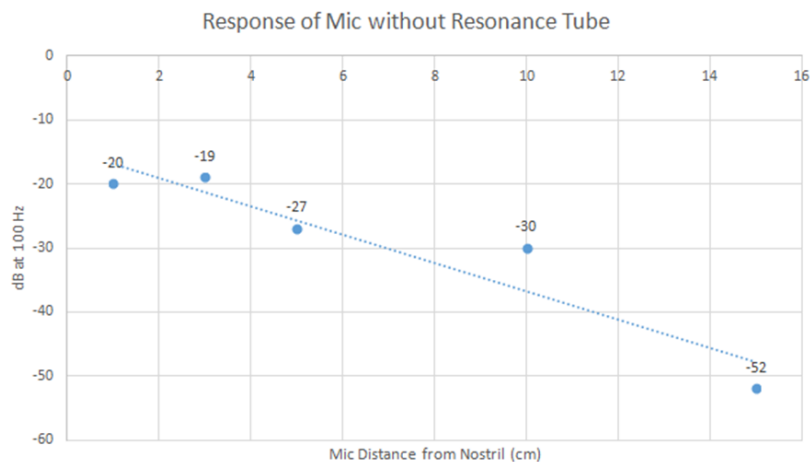


Fig. 5. The dB at 100 Hz of microphone with no resonance tube placed at different distance from the nostril.

Figure 5 shows that signal power will decrease significantly as the distance of microphone from the nostril becomes larger and after the distance of 15 cm, the microphone can hardly catch any breath sound.

But for microphone performance testing with resonance tube, this is different. The spectrum plot shows resonance with odd number harmonic frequency as example shown in Fig. 6, Fig. 7 and Fig. 8.

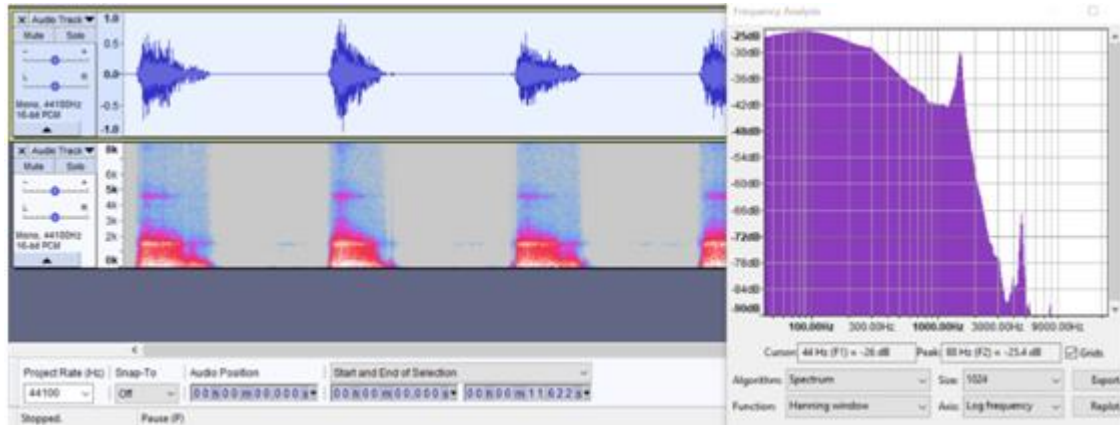


Fig. 6. Typical example of spectrum plot of microphone with short resonance tube (the case of $L = 5.5$ cm).

Figure 6 shows spectrum plot typical of resonance tube with length shorter than 10 cm where the dB at the resonance frequencies is less than the dB at lower frequency, thus shows no significant effect on enhancing the performance of microphone. The performance of the microphone depends solely on the dB at lower frequency where resonance does not occur. But when the length of resonance tube is longer than 10 cm, the dB at the fundamental resonance frequency is stronger than the dB at lower frequency and becomes dominant, thus shows significant effect on enhancing the performance of the microphone as an example shown in Fig. 7.

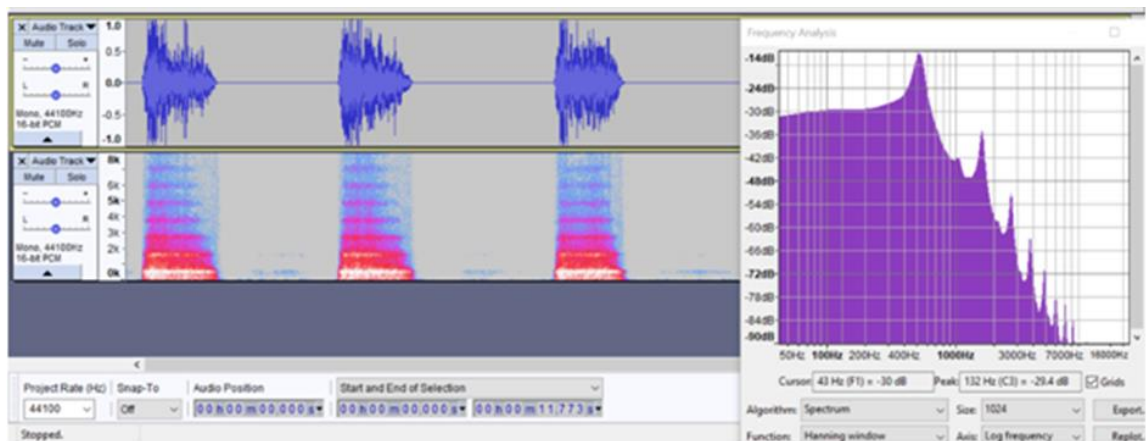


Fig. 7. Typical example of spectrum plot of microphone with long resonance tube (the case of $L = 10.5$ cm).

When the length of the resonance tube becomes much longer than 10 cm, not only the dB at the fundamental resonance frequency, but also the dB of its harmonics will help reinforce the sound pressure inside the tube, thus enhance the performance of the microphone as an example shown in Fig. 8.

The time-frequency spectrogram in Fig. 6, Fig. 7 and Fig. 8 shows vividly the power changing at fundamental resonance frequency and its harmonics along with the time during the respiration cycle which is in good agreement with the spectrum plot.

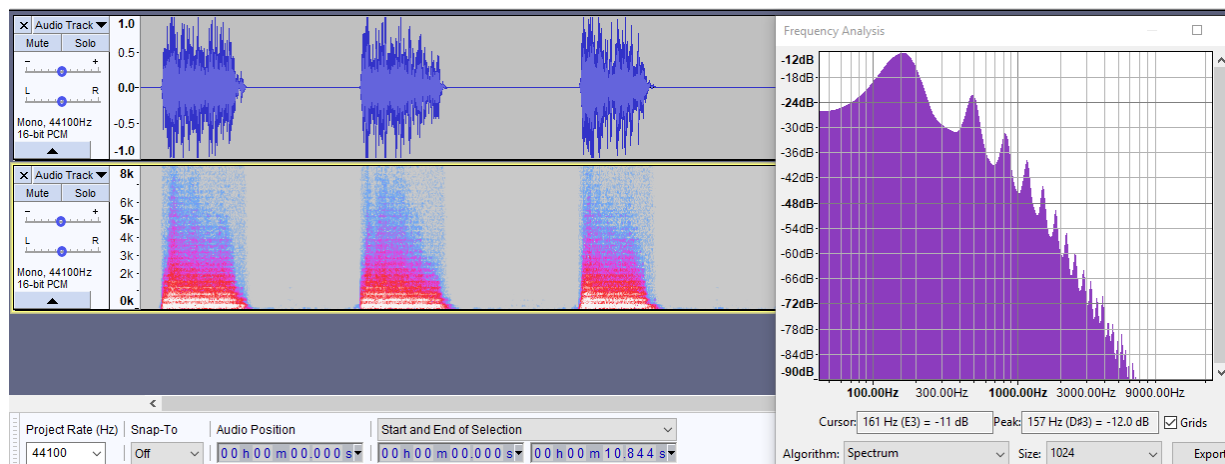


Fig. 8. Typical example of spectrum plot of microphone with longer resonance tube (the case of $L = 52$ cm).

The dB at fundamental frequency of microphone with resonance tube is plotted against the length of resonance tube to show its contribution in enhancing the performance of the microphone as in Fig. 9.

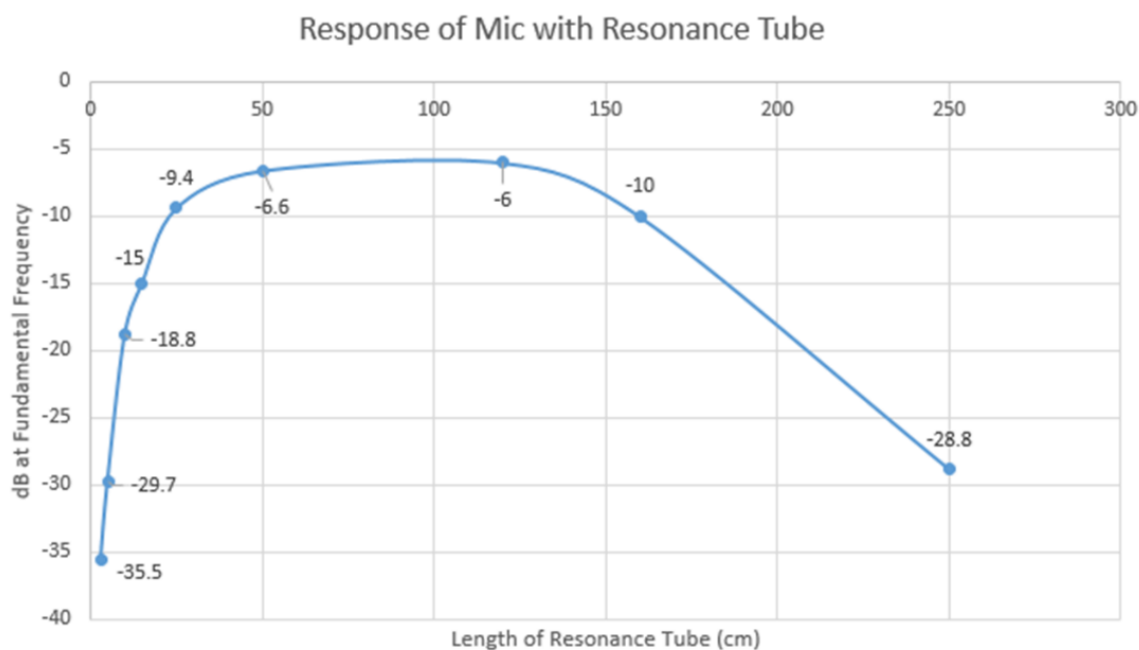


Fig. 9. The dB at fundamental frequency of microphone with resonance tube at different length.

Figure 9 shows that with longer length of resonance tube, the dB at fundamental frequency become dominant and stronger than the one with no resonance which means that microphone with resonance tube is more capable of catching breath sound at much longer distance than that of microphone without resonance tube. The length of resonance tube can be as long as 250 cm with little pressure drop as tested with nasal cannula as in Fig. 10.

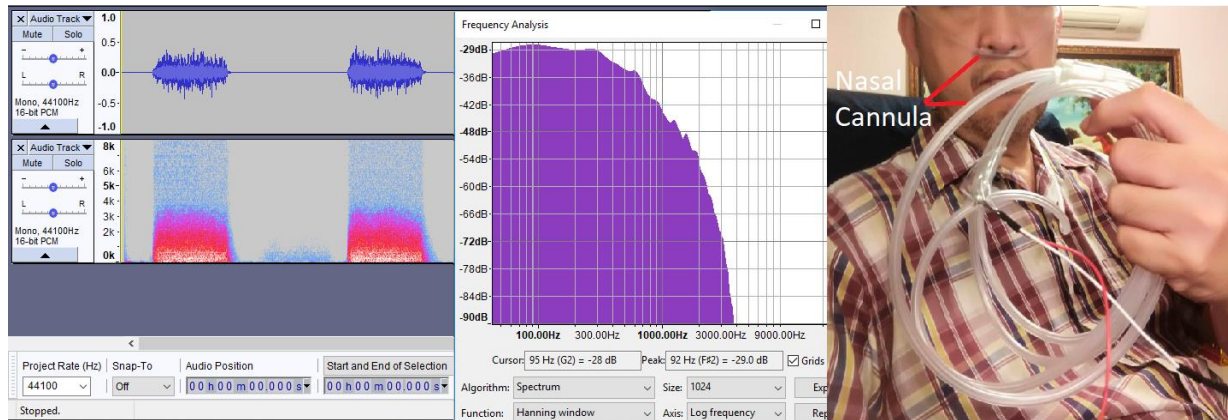


Fig. 10. Spectrum plot of microphone with resonance tube tested with nasal cannula of length 250 cm.

Figure 10 shows that with nasal cannula of length 250 cm. used as resonance tube, the resonance frequency is very low and the odd harmonic frequencies come close together which make them show no distinguished power difference. Nevertheless, with the pressure reinforcement from resonance frequency, the performance of microphone is improved and can detect breath sound as far as 250 cm. with little pressure drop.

The fundamental frequency and its harmonics at different lengths of resonance tube are calculated and compared with the measured value from spectrum plot and is shown in Table 2.

Table 2. Comparison of fundamental frequency and odd harmonic frequencies for the third, the fifth and the seventh for different lengths of tube.

Tube Length (cm)	Wave Length (cm)	F1(Calcu) Hz	F1(Meas) Hz	Error (%)	F3(Calcu) Hz	F3(Meas) Hz	Error (%)	F5(Calcu) Hz	F5(Meas) Hz	Error (%)	F7(Calcu) Hz	F7(Meas) Hz	Error (%)
3.3	13.2	2598	2518	3.10	7795	7900	-1.34	12992	-	-	18189	-	-
5.5	22	1559	1508	3.28	4677	4582	2.04	7795	8078	-3.62	10914	-	-
10.5	42	817	780	4.49	2450	2386	2.61	4083	3987	2.36	5717	5582	2.36
16	64	536	519	3.16	1608	1597	0.67	2680	2681	-0.05	3752	3759	-0.20
20	80	429	407	5.07	1286	1305	-1.46	2144	2119	1.15	3001	2938	2.11
26	104	330	322	2.37	989	983	0.65	1649	1643	0.37	2309	2325	-0.71
52	208	165	157	4.79	495	489	1.15	825	823	0.18	1154	1160	-0.49
125	500	69	64	6.71	206	195	5.25	343	332	3.21	480	466	2.96
170	680	50	43	14.75	151	147	2.86	252	245	2.86	353	345	2.29

Table 2 shows the compliance between theoretical value and measured value of the fundamental frequency and odd harmonic frequencies for the third, the fifth and the seventh for different lengths of tube. The error is mostly under 5 % for all harmonic frequencies at all lengths of tube with the exception for the fundamental frequency of the length 125 and 170 cm whose errors are 6.71 and 14.75 % respectively. This can be attributed to the bending effect in the case of long tube [14]. But so far as respiratory rate is concerned, this error lends no effect to the developed device. The lengths of tube are adjusted to represent the actual length between the open end to the surface of the microphone. Besides, the fundamental frequency and odd harmonic frequencies for the nasal cannula of length 250 cm is excluded from the Table 2 as the resonance frequency is very low and the odd harmonic frequencies come close together which make it difficult to measure accurately.

3.2. Signal Pre-Processing Unit

Breath sound signal comprises inspiration period and expiration period with pause between them. Breath sound measurement over the trachea with microphone shows nearly the same amplitude between inspiration and expiration. The smooth beginning with abrupt ending is often found during the inspiration period while abrupt beginning and smooth ending is obvious during expiration period [15]. In the case of breath sound directly measured from the mouth and/or nostril using resonance tube developed in this paper, breath sound travels into the tube during expiration, but very little sound can get into the tube during inspiration due to the tube's wall and the closed end which shields inspiration sound and environmental noise from entering the tube to the microphone. Although the microphone used in this paper is omnidirectional, but it performs like a unidirectional microphone due to the configuration. This makes breath sound signal from the microphone shows only expiration period and nearly quiet period alternatively. In order to measure respiration rate from expiration sound, signal pre-processing unit is designed comprising amplifier circuit, envelope detector circuit, and comparator circuit. The low-cost off-the-shelf LM324 quad op-amp is used for this purpose.

3.2.1. Experimental setup

Breath sound signal from microphone is fed into the amplifier circuit with gain = 100 through a DC blocking capacitor, after which the output from amplifier circuit is passed into the envelope detector circuit. The output from envelope detector circuit is then fed into the non-inverting input of comparator circuit while suitable reference voltage (0.25 V) is fed to the other input. The breath sound signal from the microphone, the outputs of amplifier circuit, envelope detector circuit and comparator circuit are measured with oscilloscope as shown in Fig. 11. Channel 1 is set to be 100 mV/div with the rest of the channels set at 5 V/div. Time scale is 2 s/div for all channels.

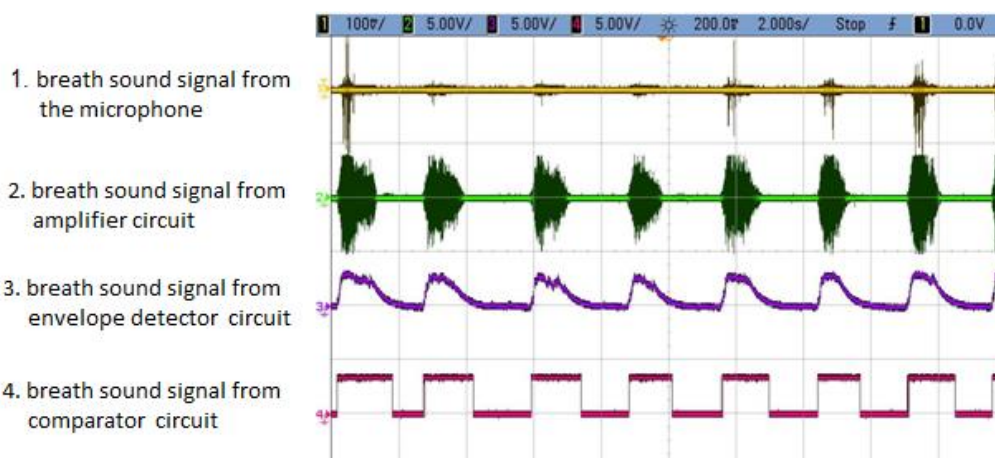


Fig. 11. Breath sound signal from the microphone, amplifier circuit, envelope detector circuit and comparator circuit (resonance tube of length 50 cm).

3.2.2. Experimental result

Figure 11 shows an example of the 4-channel oscilloscope displaying breath sound signal from the microphone and the outputs of amplifier circuit, envelope detector circuit and comparator circuit (resonance tube of length 50 cm). With different level of breathing, the breath sound signal from the microphone changes between around 10 mV (weak shallow breathing) to around 40 mV (strong deep breathing). The output of amplifier circuit will change accordingly with gain=100 from around 1 V to around 4 V where it is saturated

and the peak of output signal from envelope detector circuit will change between around 1 V to around 3.5 V. The time constant of envelope detector circuit is designed to be $4.7 \mu\text{F} * 80 \text{k}\Omega = 0.376 \text{ s}$ in order that it will be short enough to follow the rising pulses of high frequency breath sound signal which is around 1 kHz, but long enough not to fall too quickly between each high frequency pulses during expiration period. The last signal in channel 4 is the output of comparator circuit which is square wave pulse train synchronized with the respiratory cycle. The amplitude of the pulse train is saturated at around 4 V which is enough to be used as digital signal to feed into the microcontroller of the data analysis and display unit.

It can be said that most of the time the square wave signal from comparator circuit synchronizes with the respiratory cycle and presents respiratory rate accurately. But it was found in later state that there are situations when the expiration becomes unstable and fluctuates, resulting in untimely square wave pulse which causes error in the respiratory rate calculation as shown in Fig. 12. Another situation is noises from body movement which can cause artefact during the inspiration and pause period as also shown in Fig. 12.

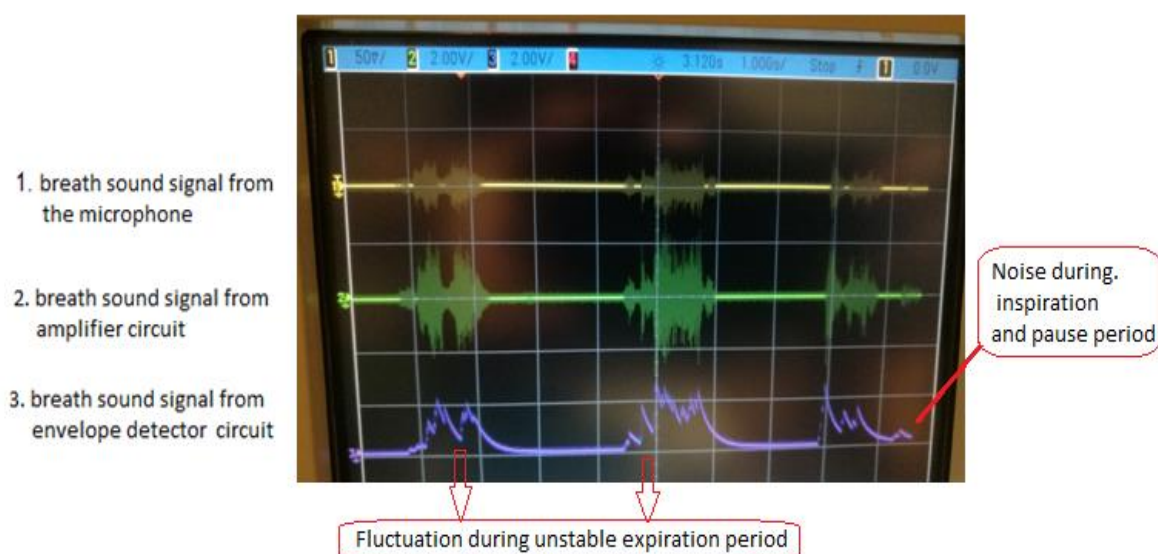


Fig. 12. Causes of errors and noises during the respiratory cycle.

In order to measure the respiratory rate accurately, reference voltage (V_{ref}) should be low enough (lower than the minimum point of fluctuation) during the expiration period, and reference voltage (V_{ref}) should be high enough (higher than the maximum point of noises) during the inspiration and pause period. Usually, inventors will try to solve this problem by compromising the contradictory requirements with trade-off or optimization method. But this is not a breakthrough solution. This situation is called “Inventive situation” in the Theory of Inventive Problem Solving (TRIZ) [16] which states that in order to attain an ideal solution, contradiction must be overcome with no trade-off or compromising by utilizing resources within or in the environment of the system at no or little cost [17]. This kind of contradiction is called physical contradiction and the solution ideas can be generated by principle of separation which is divided into separation in space, in time, in system, and by condition [18]. In this case, it is more practical to generate ideas from the concept of separation in time, that is V_{ref} must be low during expiration period and V_{ref} must be high during inspiration and pause period. In order to attain an ideal solution, we look into the system and discover that the microcontroller (PIC16F628A) which is used for data analysis can be utilized to get different value of V_{ref} during different period of time. Thus we write a source code with C language to differentiate between expiration period and outside expiration period (inspiration and pause period) and send different V_{ref} from microcontroller to the comparator circuit. The output from envelope detector circuit is fed into the non-inverting input of comparator circuit while reference voltage is fed into the other input. In order to eliminate

errors and noises, reference voltage of 0.21 V during expiration period and 1.25 V outside the expiration period is generated and applied alternatively as shown in Fig. 13.

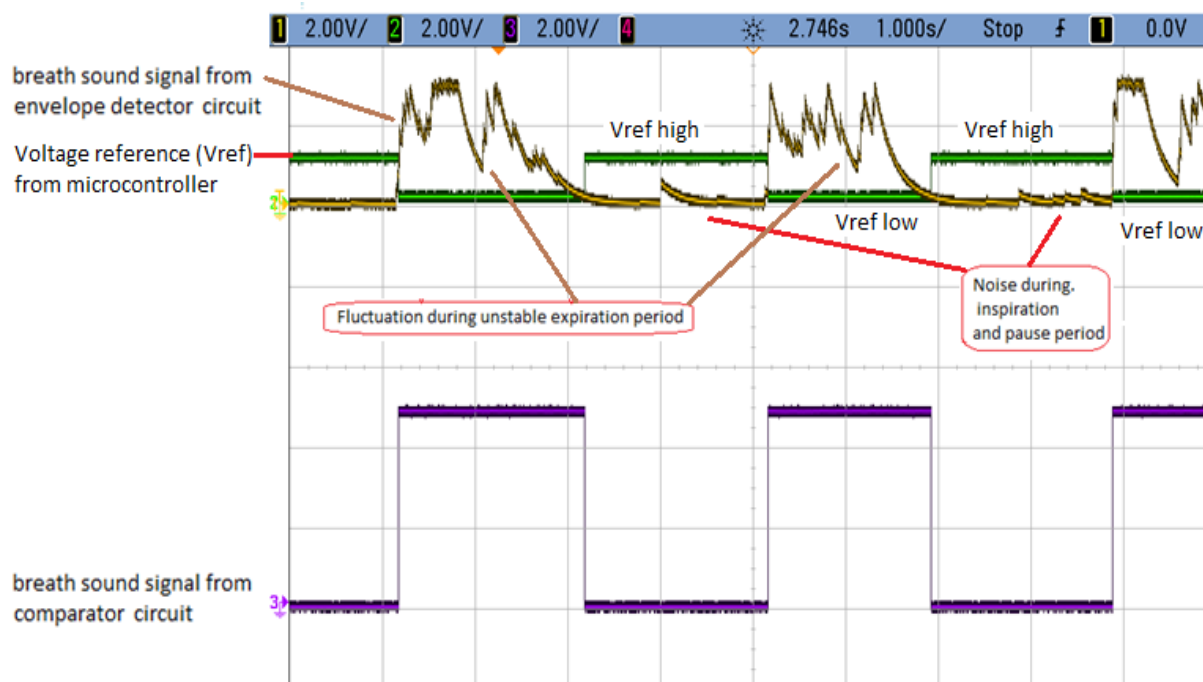


Fig. 13. Envelope of breath sound signal compared with adaptive voltage reference.

From Fig. 13, it can be seen that the designed code works well to give different voltage reference for different period of respiratory cycle. The voltage reference adjusts itself to be low to evade the fluctuation during unstable expiration period, and floats high above the noises during inspiration and pause period. The output from the comparator is a clean square wave with no errors and artefact which is forwarded to the data analysis and display unit in the following section.

3.3. Data analysis and Display Unit

Data analysis and display unit is made of PIC16F628A microcontroller and 16x2 LCD. PIC16F628A is a small microcontroller with limited I/O port, memory, and features, but it has sufficient capacity for analysing and displaying the data. The internal 4 MHz of oscillator is utilized to lessen part count and the built-in feature of CCP is deployed to detect the rising edges of the pulse train of square wave in order to calculate the breath rate per minute. The result of breath rate per minute calculated from each two consecutive rising edges of square wave along with the status of breathing as in Table 1 is displayed on 16x2 LCD.

3.3.1. Experimental setup

To verify the accuracy of the data analysis and display unit, the two input signals and output signal of the comparator circuit are simultaneously displayed on the digital storage oscilloscope (Agilent Technology) and breath rate per minute of the last two consecutive rising edges of square wave on the oscilloscope is calculated manually and compared with that displayed on the LCD as in Fig. 14. (The experiment is carried out with deep and stable breathing in order that no fluctuation of expiration period is to be worried about and the voltage reference for comparator circuit is kept constant at 1 V).

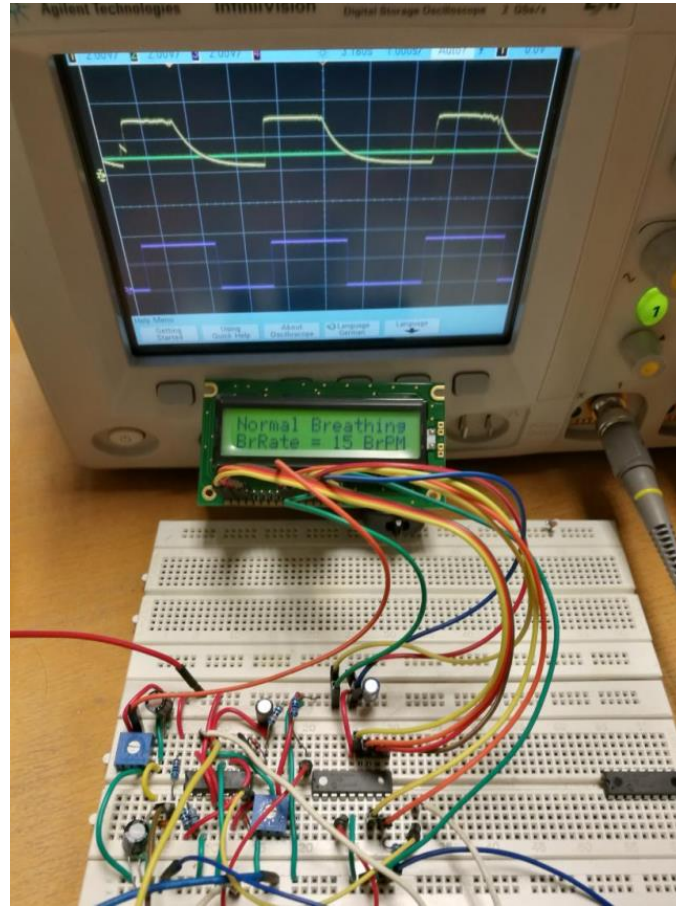


Fig 14. Verification of data analysis and display unit.

3.3.2. Experimental result

Different speeds of respiratory cycle are blown into the microphone with resonance tube of length 50 cm and the breath rate per minute calculated manually from oscilloscope ($\text{BrPM} = 60/\text{Period}$) are compared with the breath rate per minute from the LCD as in Fig. 14 and the result is shown in Table 3.

Table 3. Comparison of breath rate per minute.

Speed of respiratory cycle	Fast	Normal	Slow	Critical	No breathing
Period (s, calculated)	2.7	3.9	6.6	17	65
Breath per minute (calculated)	22.2	15.4	9.1	3.5	0.9
Breath per minute (displayed on LCD)	22	15	9	3	0

Table 3 shows that the data analysis and display unit gives an accurate breath rate per minute as designed. The respiratory rate is designed to round up to the floor of the value calculated from the period of the two consecutive rising edges of square wave synchronized with respiratory cycle. The reason is for safety as can be seen in the case of no breathing in Table 3 where the respiratory rate calculated from the period of the

two consecutive rising edges is 0.9, if it is rounded up to the ceiling of the value, it will be one breath rate per minute which may cause error in the interpretation and become too optimistic.

3.4. Performance Testing of the Whole System

After testing and fine-tuning of each units (gain of amplifier circuit changes from 33 to 100, time constant of envelope detector circuit from 0.47 s to 0.24 s, and reference voltage of comparator circuit from constant value of 1 V to dynamic value of $V_{ref}(\text{low}) = 0.21 \text{ V}$ and $V_{ref}(\text{high}) = 0.83 \text{ V}$), the performance of the entire system is tested and compared with well-known respiratory rate monitoring device called capnography [19] which detects end tidal CO_2 density at the end of each expiration period. Capnography is normally used in intensive care unit and sleep study center [20] and is usually considered as gold standard for respiratory rate measurement.

3.4.1. Experimental setup

The respiratory rate is measured simultaneously with the developed device using microphone with resonance tube and the capnography device using a non-dispersive infrared end tidal CO_2 sensor (Mainstream Et CO_2 , Wuhan Cubic Optoelectronics). The open end of the resonance tube is placed inside the airway adapter below the sensor not to obstruct the infrared beam. Different speed and level of respiratory cycles are blown directly from the mouth through the airway adapter and respiratory rate are measured simultaneously from the LCD and the capnography displayed on the notebook as shown in Fig. 15.

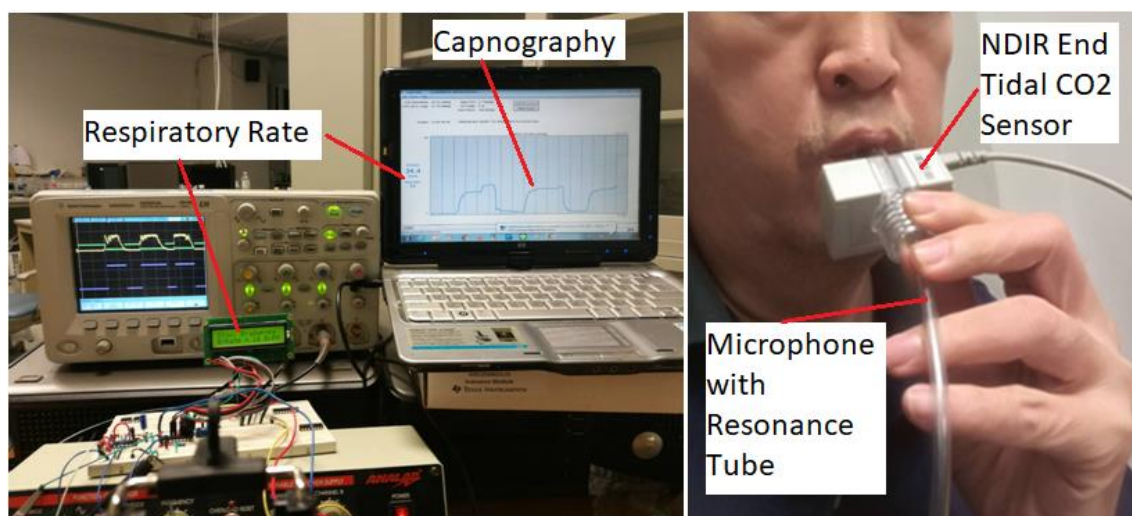


Fig. 15. Comparison of respiratory rate monitoring device between microphone with resonance tube and capnography device

3.4.2. Experimental result

The respiratory rate measured with the developed device using microphone with resonance tube results in good agreement with that measured with capnography device using a non-dispersive infrared end tidal CO_2 sensor as an example shown in Fig. 16.

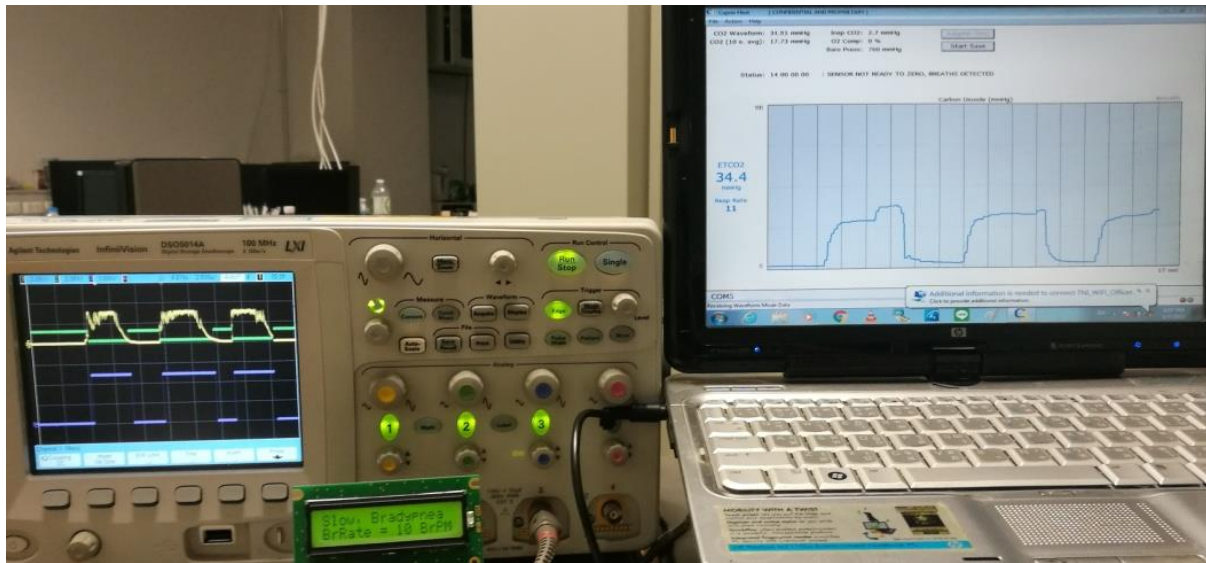


Fig. 16. Example of comparison between respiratory rate measured with the developed device (on LCD) and with capnography device (on the PC).

From Fig. 16, the respiratory rate measured with the developed device reads 10 Breaths per minute (BrPM) while that with capnography device reads 11 BrPM. The 1 breath error can be attributed to the difference in the algorithm for calculating respiratory rate of the two devices. For the developed device using microphone with resonance tube, respiratory rate is calculated from the rising edges of the square wave pulse train pre-processed to be synchronized with the respiratory cycle. For the capnography device, respiratory rate is calculated from the end tidal CO_2 density, thus it has to wait until the end of expiration period before the respiratory rate can be calculated. Therefore, the present value of 11 BrPM of the capnography device will be the previous value of the developed device using microphone with resonance tube as can be calculated from the period between the first and second rising edges. It can be concluded that the capnography device using non-dispersive infrared end tidal CO_2 sensor responds to changes slower than the developed device using microphone with resonance tube. From the experiment with other different speed and level of respiratory cycles blown directly from the mouth through the airway adapter, the results show that after the respiratory rate reaches constant value, both devices will show the same BrPM as shown in Fig. 17 - Fig.20.

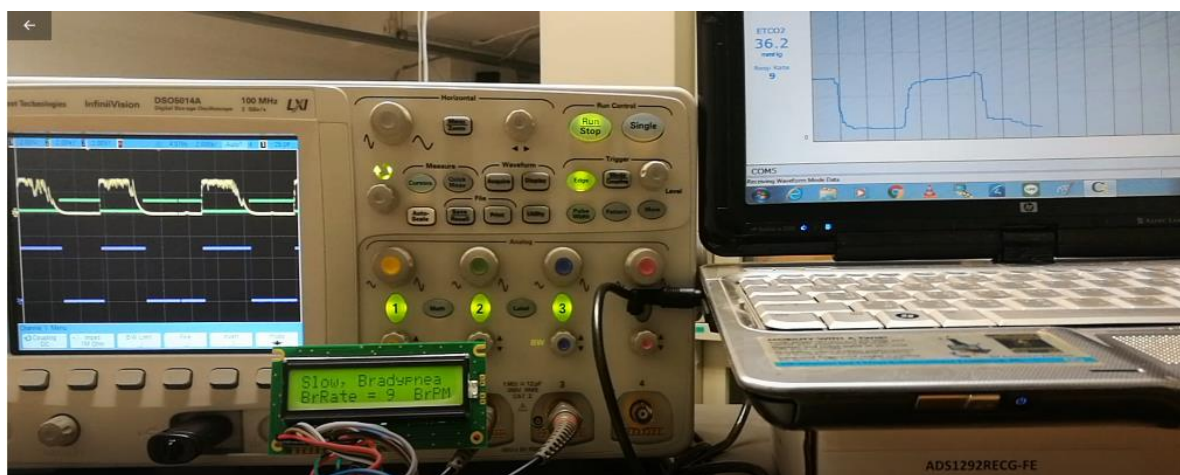


Fig. 17. Comparison between respiratory rates measured with the developed device and with capnography device at slow breathing (9 BrPM).



Fig. 18. Comparison between respiratory rates measured with the developed device and with capnography device at normal shallow breathing (15 BrPM).



Fig. 19. Comparison between respiratory rates measured with the developed device and with capnography device at fast breathing (22 BrPM).



Fig. 20. Comparison between respiratory rates measured with the developed device and with capnography device at very fast breathing (98 BrPM).

The results of performance test in Fig. 17 - Fig. 20 show that respiratory rates measured with the developed device have the same value as those measured with capnography device. The results can be summarized as bar chart in Fig. 21 to compare the breath rate per minute (BrPM) at different speeds of respiratory cycle between the developed device and with capnography device which results in the same value.

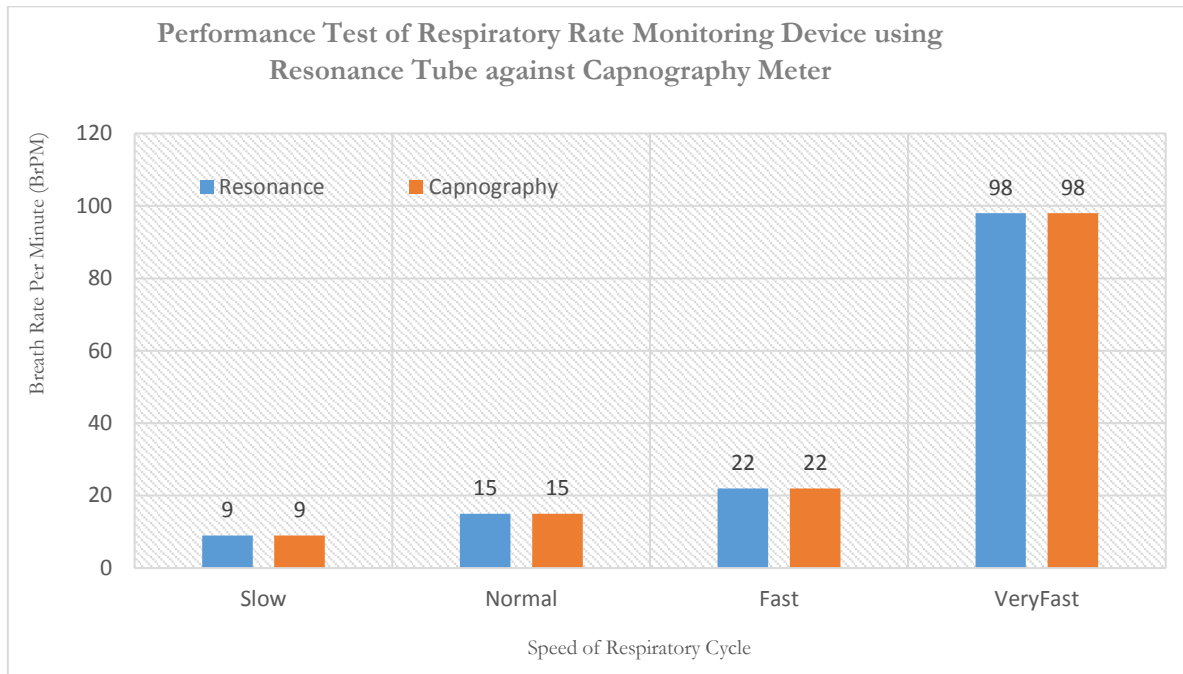


Fig. 21. Performance Test of Respiratory Rate Monitoring Device using Resonance Tube against Capnography device.

4. Discussion and Conclusion

The respiratory rate measuring device developed in this paper uses resonance effect of resonance tube to enhance the performance of microphone which, to the best of our knowledge, has never been studied before. The distance that breath sound can reach microphone is much longer with resonance tube than without it. Recent study on respiratory rate estimation using built-in microphone of a smartphone shows that nasal sound can be accurately estimated as far as 30 cm away from the nose [21]. But with the enhancement from resonance effect of resonance tube, the microphone in the device developed in this paper can catch breath sound in the tube with normal breathing as far as 250 cm as already tested with nasal cannula as shown in Fig. 10.

Besides, this device can tolerate noises to the extent that it needs no complicated filtering system as is required in the cases of using built-in microphone of a smartphone [21] or using stethoscope-like chest piece made of microphone to detect respiratory sound via chest wall or the skin over trachea which are prone to noise from inside and outside the measured object [22]. The respiratory rate measuring device developed here uses a simple algorithm to evade noise inside and outside the system by overcoming the contradictory requirement of reference voltage value for the comparator circuit (V_{ref} must be low during expiration period and must be high outside expiration period, details as described in 3.2). Usually, this kind of problem is solved using trade-off or compromised with optimization method which cannot eliminate the source of noise completely and will need a filtering system in the latter state. It is the first time, also to the best of our knowledge, that this contradictory requirement is overcome without compromise by deploying the principle of separation in TRIZ [18] by generating low reference voltage during expiration period and high reference

voltage outside expiration period. This prevents errors from unstable expiration breath sound during expiration period and evades noise and artefact during inspiration and pause period as shown in Fig. 18.

From Fig. 18, it is obvious that respiratory rates measured with the developed device can perform accurately compared with capnography device even in the case of shallow breathing of which the breath sound signal is very weak (10 mV) and full of fluctuation (yellow colour line). With the help of adaptive reference voltage (green colour line), no untimely square wave is mistakenly created during expiration period and no artefact square wave is erroneously created by noises during inspiration and pause period as happens between the second and the third breath in Fig. 18.

We believe that this new approach of respiratory rate measurement using resonance tube and the creative noise evasion procedure will be useful and applicable to clinical diagnosis and health concerned society.

Future work will be done to enhance the system to mobile application and to relate the amplitude of breath sound signal to airflow volume in order that it can measure airflow at shallow breathing or hypopnea which is necessary to calculate Apnea and Hypopnea Index (AHI) in sleep study.

References

- [1] D. Evans, B. Hodgkinson, and J. Berry, "Vital signs in hospital patients: A systematic review," *International Journal of Nursing Studies*, vol. 38, no. 6, pp. 643–650, 2001.
- [2] M. A. Cretikos, R. Bellomo, K. Hillman, J. Chen, S. Finfer, and A. Flabouris, "Respiratory rate: The neglected vital sign," *Med. J. Aust.*, vol. 188, no. 11, p. 657, 2008.
- [3] T. Neideen, "Monitoring devices in the Intensive Care Unit," *Surgical Clinics of North America*, vol. 92, no. 6, pp. 1387–1402, 2012.
- [4] F. Barbieri, W. Dichtl, E. Brandauer, A. Heibreder, A. Stefani, A. Adukauskaitė, and B. Hoegl, "Sleep apnea detection by a cardiac resynchronization device integrated thoracic impedance sensor—A validation study against the gold standard polysomnography," *EP Europace*, vol. 20, no. suppl_1, pp. i146–i146, 2018.
- [5] T. L. Jacobs, E. S. Epel, J. Lin, E. H. Blackburn, O. M. Wolkowitz, D. A. Bridwell, and C. D. Saron, "Intensive meditation training, immune cell telomerase activity, and psychological mediators," *Psychoneuroendocrinology*, vol. 36, no. 5, pp. 664–681, 2011.
- [6] T. Benjaboonyazit, "Searching for innovative respiratory rate monitoring devices: A case study and review of TRIZ Standard Solutions Class 4 and MAR Operator," in *Proceedings of the 2018 International Conference on Systematic Innovation*, July 19–21, 2018.
- [7] A. K. Gupta, "Respiration rate measurement based on impedance pneumography," Texas Instruments Application report SBAA181–February, 2011.
- [8] P. Pitiphok, "Design and implementation of respiratory inductive plethysmography," M.Eng. thesis, Department of Electrical Engineering, Faculty of Engineering, Chulalongkorn University, Bangkok, Thailand, 2011.
- [9] F. Q. AL-Khalidi, R. Saatchi, D. Burke, H. Elphick, and S. Tan, "Respiration rate monitoring methods: A review," *Pediatric Pulmonology*, vol. 46, no. 6, pp. 523–529, 2011.
- [10] S. Ohshimo, T. Sadamori, and K. Tanigawa, "Innovation in analysis of respiratory sounds," *Annals of Internal Medicine*, vol. 164, no. 9, p. 638, 2016.
- [11] P. Corbishley and E. Rodriguez-Villegas, "Breathing detection: Towards a miniaturized, wearable, battery-operated monitoring system," *IEEE Transactions on Biomedical Engineering*, vol. 55, no. 1, pp. 196–204, 2008.
- [12] P. Forgacs, A. R. Nathoo, and H. D. Richardson, "Breath sounds," *Thorax*, vol. 26, pp. 288–295, 1971.
- [13] H. Pasterkamp, S. S. Kraman, and G. R. Wodicka, "Respiratory sounds advances beyond the stethoscope," *American Journal of Respiratory and Critical Care Medicine*, vol. 156, no. 3, pp. 974–987, 1997.

- [14] S. Félix, J.-P. Dalmont, and C. J. Nederveen, "Effects of bending portions of the air column on the acoustical resonances of a wind instrument," *The Journal of the Acoustical Society of America*, vol. 131, no. 5, pp. 4164-4172, 2012.
- [15] P. Hult, B. Wranne, and P. Ask, "A bioacoustic method for timing of the different phases of the breathing cycle and monitoring of breathing frequency," *Medical Engineering & Physics*, vol. 22, no. 6, pp. 425-433, 2000.
- [16] S. D. Savransky, *Engineering of Creativity. Introduction to TRIZ Methodology of Inventive Problem Solving*. Boca Raton, Florida: CRC Press, 2000.
- [17] D. Cavallucci, F. Rousselot, and C. Zanni, "Linking contradictions and laws of engineering system evolution within the TRIZ framework," *Creativity and Innovation Management*, vol. 18, no. 2, pp. 71-80, 2009.
- [18] T. Benjaboonyazit, "Systematic approach to problem solving of low quality arc welding during pipeline maintenance using ARIZ (algorithm of inventive problem solving)," *Engineering Journal*, vol. 18, no. 4, pp. 113-134, 2014.
- [19] J. Nagler and B. Krauss, "Capnography: A valuable tool for airway management," *Emergency Medicine Clinics of North America*, vol. 26, no. 4, pp. 881-897, 2008.
- [20] T. F. Morley, "Capnography in the intensive care unit," *Journal of Intensive Care Medicine*, vol. 5, no. 5, pp. 209-223, 1990.
- [21] Y. Nam, B. A. Reyes, and K. H. Chon, "Estimation of respiratory rates using the built-in microphone of a smartphone or headset," *IEEE Journal of Biomedical and Health Informatics*, vol. 20, no. 6, pp. 1493-1501, 2016.
- [22] S. Cortes, R. Jane, A. Torres, J. A. Fiz, and J. Morera, "Detection and adaptive cancellation of heart sound interference in tracheal sounds," presented at *2006 International Conference of the IEEE Engineering in Medicine and Biology Society*, 2006.